International Scientific Colloquium
Modelling for Electromagnetic Processing
Hannover, October 27-29, 2008

Model experiments on macroscopic thermoelectromagnetic convection

A. Cramer, X. Zhang, and G. Gerbeth

Abstract

Thermoelectromagnetic convection (TEMC) in a shallow square layer of liquid metal was investigated experimentally. The most prominent features of the setup were an as homogeneous as possible temperature gradient, a strongly inhomogeneous magnetic field, and a large value of the Seebeck coefficient. Ultrasound Doppler measurements of the flow field showed that, even at relatively small temperature gradients, a quite distinct TEMC is accomplishable if the setup is optimised with respect to the Lorentz force.

Introduction

The interaction between a thermoelectric current $\boldsymbol{j}$ and an imposed magnetic field $\boldsymbol{B}$ may produce thermoelectromagnetic convection (TEMC). Prerequisite for $\boldsymbol{j}$ is a temperature gradient ∇T and a spatial variation of the thermoelectric power S, both of which in combination may generate an electro-motive force (emf). In his pioneering study [1], Shercliff generalised Ohm's law for conducting liquids by introducing a term for the emf

$$\boldsymbol{j}/\sigma = \boldsymbol{E} + \boldsymbol{v} \times \boldsymbol{B} - S\nabla T.$$

σ, $\boldsymbol{v}$, and $\boldsymbol{E}$ are electrical conductivity of the liquid metal, velocity at which it moves, and electric field, respectively. In a system in which $\boldsymbol{v} \times \boldsymbol{B}$ is negligibly small, which is the case in almost any relevant application, and $\boldsymbol{E}$ is irrotational, the latter implying $\boldsymbol{E} = -\nabla \Phi$ with electric potential Φ, Ohm's law simplifies to

$$\boldsymbol{j}/\sigma = -\nabla \Phi - S\nabla T. \tag{1}$$

Considering any arbitrary temperature distribution in a medium of uniform composition in (1) shows that no current flows because $S\nabla T$ is also irrotational. This is due to S being a function of T only, a consequence of which is that $\nabla \mathrm{S} \times \nabla T$ vanishes. In order to have thermoelectric current flowing, $\nabla \mathrm{S}$ and ∇T must not be parallel. This is, in general, achieved by a spatially varying composition. Although these basics of TEMC are known for a long time, embodiments for a significant stirring of a liquid metal pool are badly missing. This prompted us to perform an experimental study on TEMC in a generic configuration, which is concerned with the case that was termed by Shercliff as "the extreme case when the composition and S vary discontinuously across an interface along which T varies."

While the necessary temperature gradient $S \cdot \nabla T$ in a square box was established by heating and cooling of two opposing sidewalls, respectively, utilising a massive nickel plate

for the bottom of the electrically conducting container established a material discontinuity with respect to the liquid metal layer

1. Implementation of the experiment

The task formulation of a marked TEMC may be accomplished with a strong inhomogeneity of the magnetic flux density $\boldsymbol{B}$. Since the availability of strong cobalt-samarium magnets, the demand of an inhomogeneous field is easily fulfilled with a permanent magnet made from such material having a size adapted to the dimensions of the container. The bar magnet was 50 mm in length, 20 mm in height, and 8 mm in width. With the direction of magnetisation along the shortest side, the magnet produced B = 1.1 T at its surface. The experimental setup is shown in Fig. 1. Sizes of the container are length = width = 15 cm and height = 6 cm. All four sidewalls were made from copper plates with $S \approx 2$ μV/K. The decision for the wall material was motivated by the high thermal conductivity, which approximates best what is commonly referred to as an isothermal wall. For the reason of having a high difference in the Seebeck coefficient, nickel was chosen as the bottom material having the relatively high thermoelectric power of S = 15 μV/K. A thickness of the bottom plate of 3 mm was sufficient to keep the Ohmic losses small thanks to an electrical conductivity that is significantly higher than that of the liquid metal. In order to create the temperature gradient within the electrically conducting fluid, one of the sidewalls was heated electrically, and the opposing wall was cooled with water at a high flow rate. The ternary alloy GaInSn was chosen as the melt under investigation for several reasons. Firstly, it is liquid at room temperature (T_{melt} = 10 °C) and thus convenient to handle. Secondly, GaInSn has a relatively high electrical conductivity ($\sigma_{GaInSn} = 3.27 \cdot 10^6$ $(\Omega \cdot m)^{-1}$) among the low melting point alloys, thus rendering the Ohmic losses fairly small. Thirdly, the thermo-emf $S_{GaInSn} \approx 1$ μV/K (value taken from [2]) differs not that much from the copper walls. Although the TEMC in the experiments in [2] was born of this small difference, it might be neglected here against $S_{Ni} - S_{GaInSn}$. If the driving force of TEMC is mainly located at one interface, the outcome of the experiments is much easier to interpret.

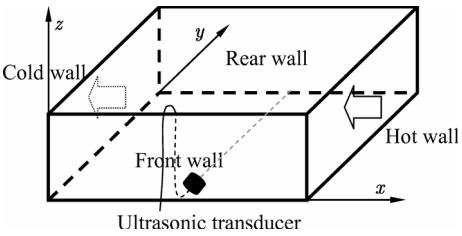

Fig. 1. Scheme of the experimental setup. A small ultrasonic transducer is located inside the liquid metal to avoid attenuation of the acoustic beam that otherwise would occur while passing the massive copper walls. The arrows indicate the direction of heat flux.

Prior filling the container with GaInSn alloy, the solid walls were pre-amalgamated. For that, relatively strong hydrochloric acid was used in combination with emery wool. A droplet of the melt was rubbed across the metallic surfaces until it completely wetted the solid. As this is necessary to have a uniform heat flux at the isothermal walls, it is even more important to ensure a good electric contact at the bottom. To protect the liquid alloy from too heavy corrosion, a thin layer of tartaric acid ($C_4H_6O_6$) covered the melt on top during the measurements. The thickness of the GaInSn layer was kept small. Thin enough to reduce buoyant convection, but thick enough to immerse a sensor for flow measurements completely. A good compromise was 15 mm. Besides observing the motion at the melt surface as in [2], local flow measurements were performed. An ultrasonic Doppler velocimeter (model DOP 2000, Signal Recovery, Lausanne/Switzerland) was used to acquire instantaneous velocity profiles along the ultrasonic beam. The principle of operation of UDV is the pulsed echo technique [3]: a time of flight measurement of an ultrasonic burst determines the location of a

scattering particle within the fluid, and the difference in time of flight measurements for consecutive bursts is a measure for the velocity of the particle travelling together with the fluid. The feasibility of liquid metal local flow measurements, in particular for recirculating flows of the GaInSn under investigation in the present work, was demonstrated in [4].

2. Results

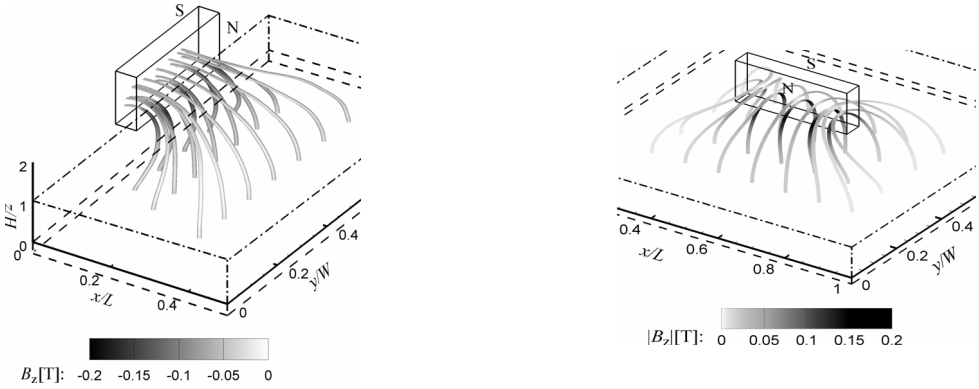

Fig. 2. Visualisation of the field of the permanent magnet. Left panel: north pole is directed toward the inner of the container, right panel: the magnet is located 5 mm above the centre of the liquid metal layer. The tubes are in alignment with the direction of the vector of magnetic flux density $\boldsymbol{B}$, and their shading corresponds to the strength of the vertical component B_z. In the right panel, the absolute value is depicted due to grey-scale presentation. The values of the tubes originating from the north pole are negative, and of those originating from the south pole are positive.

Numerical simulations were performed with the commercial solver Maxwell (Ansoft Corp.). Fig. 2 show that $\boldsymbol{B}$ is almost perpendicular to the bottom at least within the lower part of the metallic melt layer, as was to be expected because of the ferromagnetic nickel. The measurements performed with a 3-axis Gauss meter (Lakeshore, model 460 with 3D sensor MMZ-2512-UH) agreed nicely with the computations. For the following considerations, it is thus sufficient to restrict to B_z. Next, the velocities of the buoyant convection developing from ∇T were measured without the magnet. Based on these, the neglect of the $\boldsymbol{v} \times \boldsymbol{B}$-Term made above turns out as fully justified. In anticipation of the results on velocity for TEMC, it can also be stated that thermoelectricity dominates buoyancy by far.

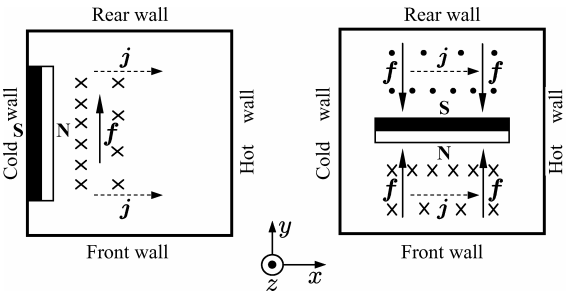

Fig. 3. Top view onto both arrangements. $\boldsymbol{j}$ flows in direction of ∇T (c. f. (1)) and since $\boldsymbol{B}$ is directed downward, the thermoelectromagnetic body force is always in y-direction; strongest at the magnet and diminishing with increasing distance.

Fig. 3 sketches the forces produced by both configurations of the magnetic field (c. f. Fig. 2) and the assumption of a homogeneous current between the isothermal walls. The coordinate system depicted at the bottom is subsequently used throughout the text. The flow structure expected to develop from the force depicted in the left panel is simple: it is a recirculation in the horizontal plane driven by the force acting in y-direction at the cold wall. The single convection cell rotates clockwise. Also the situation in the right panel is easily understandable: fluid will move from both rear and front walls toward the centre of the box and recirculate accordingly. The convective pattern will be that of four vortices in which

diagonally opposing cells have the same rolling direction. Because the cell boundaries are not rigid walls, the system with the magnet above the centre likely is the more unstable one. Free boundaries are potential sources of instability in many fluid-dynamical systems.

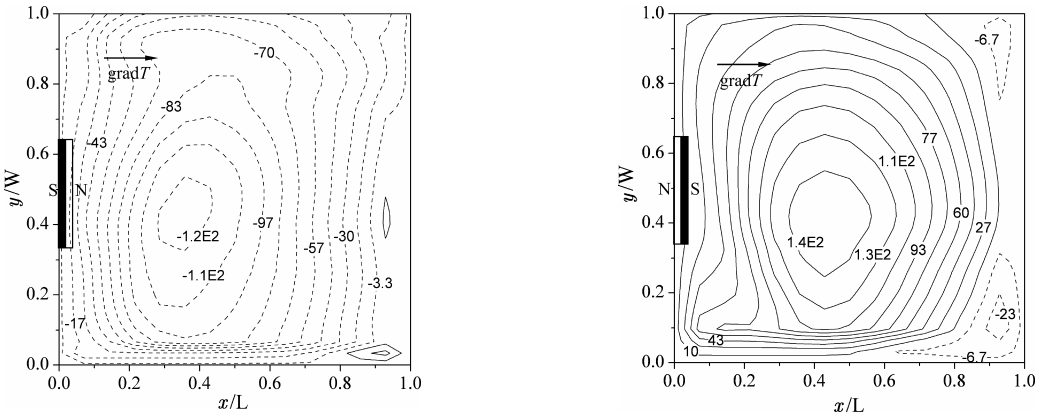

Fig. 4. Contour lines of the stream function of the time-averaged flow field for ΔT = 30 K. The long side of the magnet is aligned with the cold wall while the direction of the magnetisation in the left panel is in parallel with the temperature gradient. As can be seen from the legends of the iso-lines, the single vortex in the right panel has an opposing rolling direction while the absolute value of the stream function does not change within the precision of measurements.

UDV measurements corresponding to the left panel of Fig. 3 are comprised in Fig. 4. While controlling the temperature difference between the hot and cold wall to ΔT = 30 K, velocity profiles in one of the horizontal directions at a fixed location in the other horizontal direction were sampled for a duration of 120 seconds. Then, the ultrasonic transducer was moved by 1 cm with respect to the second coordinate. This procedure repeated until the whole area of the container was scanned. From the area-wide time-averaged mean values of velocity, a stream function may be computed. The iso-contours in the left panel of Fig. 4 correspond to the left panel of Fig. 3 as can be seen from the negative values of the stream function. The single convection cell penetrates the container entirely while the eye of the vortex is moved off centre toward the source of motion. Such topology is typical for re-circulating flows. In the right panel of Fig. 4, the polarity of the magnet is reversed and the direction of rotation changes from clockwise to counter-clockwise, accordingly.

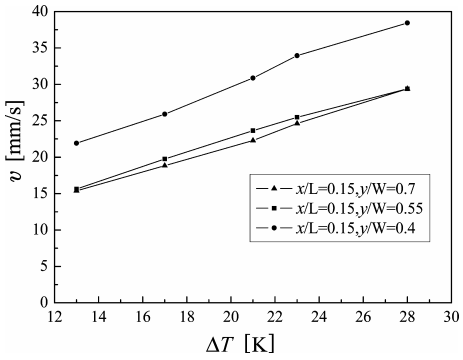

Fig. 5. Mean velocity for the configuration with the magnet at the cold wall in dependence of the temperature difference.

Remaining with time-averaged mean values, Fig.5 exemplarily shows the dependence of v on ΔT for three positions close to the cold wall. The coordinate (x = 0.15 L, y = 0.55 W) is chosen so as to have the maximum velocity measured there. The small asymmetry indicates that the imperfection of the experimental setup was also small. Both other points are in the same distance from that of highest velocity, hence the measurements agree very well. In the range up to ΔT = 28 K, the measured velocities depend linearly on ΔT, which, in turn, is proportional to the thermoelectromagnetic body force. At half the maximum possible ΔT = 25 K, the velocity

reaches a value of $v \approx 35$ mm/s. Provided that $v \propto \Delta T$ up to $\Delta T = 50$ K, a value of 70 mm/s is indeed large compared to 5 mm/s measured for the pure buoyant case for that temperature difference.

Although the flow was relatively stable to the appearance of observation with the naked eye, velocities in the range of several cm/s indicate that the flow is not laminar. A measuring location closer to the eye of the vortex is chosen for closer examination since the ratio of the intensity of the velocity fluctuations and the mean velocity is expected to be larger there than in the region of forcing. As can be seen in the time series in Fig. 6, the flow is turbulent.

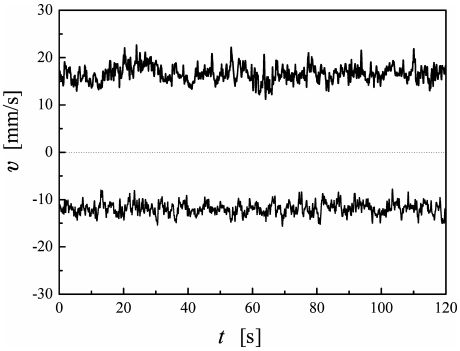

Fig. 6. Time series of the local instantaneous velocity at (x = 0.43 L, y = 0.37 W) for ΔT = 30 K. The upper curve with positive values of v corresponds to the configuration in the left panel of Fig. 3, and the lower one to the right panel.

When the magnet was located above the centre of the container, a convective pattern consisting of four cells developed as expected from the distribution of the thermoelectromagnetic body force. Also in this configuration, both orientations of the magnet, one of which was that the north pole was directed to the front wall leading to a force toward the centre and the other was that the north pole pointed to the rear wall and the force was directed away from the centre, were considered. The corresponding stream functions are to be found in Fig 7. Again, the vortices change their rolling direction when the direction of magnetisation is inverted.

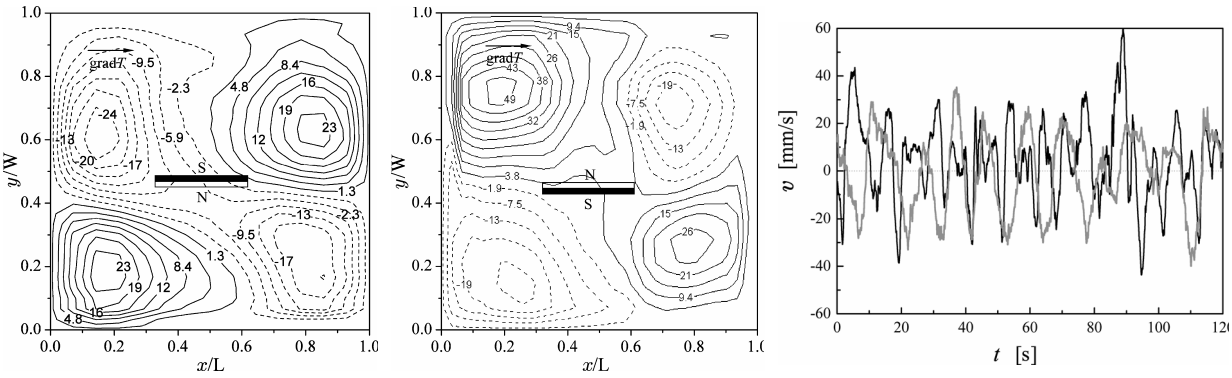

Fig. 7. Iso contours of the stream function (leftmost two panels) and time series of v at the same location as in Fig. 6 (right panel) for the magnet positioned above the centre at ΔT = 40 K. The black line shows the time series when the north pole of the magnet points to the front wall, and the grey line when the magnet is turned by 180 °.

Although the temperature difference was 10 K higher than in the case of the single cell, mean velocities decreased distinctly whereas the turbulence was significantly intensified. Besides both altered topology of the convective pattern and reduced mean velocities, also the turbulence characteristic indicates a qualitatively different flow regime. The geometry of the single cell, which is in first place the location of the vortexes eye, was relatively stable. Whatever duration the sampled velocity profiles are averaged, the mean value at any position within the profile does not change much. In contrast, the four-cell pattern was quite unstable. Mean values obtained from averaging over durations up to 20 seconds even may differ in

sign. The flow is characterised by oscillations of the mean flow eddies, which can be either movement of the vortices' eyes and/or growth and shrinkage of the vortices. Time series for both directions of the magnet are plotted in the rightmost panel of Fig. 7. Of course will any averaging tend to a mean value provided a sufficiently long period over which the average is calculated. Comparison of the time series in Figs. 6 and 7 however evidences the qualitative difference: the typical time scales of the fluctuations differ by two orders of magnitude or even more, and the large-scale pattern *oscillates* around a non-existing (zero) mean value. Intermittence was not observed in the investigated range of the TEMC-driving temperature differences.

Conclusions

Macroscopically observable thermoelectromagnetic convection (TEMC) was studied in a model experiment. Being generic to a certain extent, the geometry of a square box with a homogeneous temperature gradient between two sidewalls was chosen in conjunction with employing a small permanent magnet close to the melt surface. The crux of the experiment is that the bottom of the container was made from nickel. Whenever there is a freedom to select the material of structural components being in contact with the melt, the target should be to maximise the thermo-electro motive force with respect to the fluid if a pronounced TEMC is the objective. About 20 μV/K is quite much, this value allowed achieving a time-dependent flow regime even at the moderate temperature difference of 40 K. To the best of our knowledge, turbulent convection was the first time observed for the equivalent temperature gradient of only 2.67 K/cm.

As an input parameter to the experiment, the position of the magnet was varied leading to different distributions of the thermoelectrically generated Lorentz force. When the magnet was located close to either isothermal wall with its direction of magnetization parallel to $S \cdot \nabla T$, a single vortex developed throughout the whole container while the flow might be assessed as relatively stable. Moving the magnet to the centre modified the topology to four vortices and intensified the velocity fluctuations. The numerical results for the distribution of the magnetic field in presence of the ferromagnetic bottom support the experimental findings.

References

[1] Shercliff, J. A.: *Thermoelectric magnetohydrodynamics*. J. Fluid Mech., Vol. 91, 1979, pp. 1917-1928.

[2] Gorbunov, L. A.: *Effect of thermoelectromagnetic convection on the production of bulk single-crystals consisting of semiconductor melts in a constant magnetic field*. Magnetohydrodynamics, Vol. 23, 1987, No. 4, pp. 400-407.

[3] Takeda, Y.: *Development of an ultrasound velocity profile monitor*. Nucl. Eng. Des., Vol. 126, 1993, pp. 277-284.

[4] Cramer, A., Zhang, C., and Eckert, S.: *Local flow structures in liquid metals measured by ultrasonic Doppler velocimetry*. Flow Meas. Instrum., Vol. 15, 2004, pp. 145-153.

Acknowledgement

This work was supported by Deutsche Forschungsgemeinschaft in the framework of the collaborative research centre SFB 609 entitled “Electromagnetic Flow Control in Metallurgy, Crystal Growth and Electrochemistry.“

Authors

Dr. rer nat. Cramer, Andreas, Dr. rer nat. Zhang, Xiugang, and Dr. rer nat. Gerbeth, Gunter are all with
Department of Magnetohydrodynamics
Forschungszentrum Dresden-Rossendorf
Bautzner Landstraße 128
D-01328 Dresden, Germany
E-mail: a.cramer@fzd.de, zhangx@fzd.de, g.gerbeth@fzd.de